Title	Stress on the posteromedial region of the proximal tibia increased over time after anterior cruciate ligament injury
Author(s)	Miura, Soya; Iwasaki, Koji; Kondo, Eiji et al.
Citation	Knee surgery sports traumatology arthroscopy, 30(5), 1744-1751 https://doi.org/10.1007/s00167-021-06731-4
Issue Date	2022-05-01
Doc URL	https://hdl.handle.net/2115/89277
Rights	This is a post-peer-review, pre-copyedit version of an article published in Knee Surgery, Sports Traumatology, Arthroscopy. The final authenticated version is available online at: http://dx.doi.org/org/10.1007/s00167-021-06731-4
Type	journal article
File Information	KSSTA_ACL-CTOAM.pdf

Knee Surgery, Sports Traumatology, Arthroscopy (KSSTA)

Title: Stress on the Posteromedial Region of the Proximal Tibia Increased Over Time after Anterior Cruciate Ligament Injury

Soya Miura. M.D.[1], Koji Iwasaki. M. D., Ph. D.[2], Eiji Kondo. M. D., Ph. D.[3], Kaori Endo. M. D., Ph. D.[1], Shinji Matsubara. M. D., Ph. D.[1], Masatake Matsuoka. M. D., Ph. D.[1], Tomohiro Onodera. M. D., Ph. D.[1], Norimasa Iwasaki. M. D., Ph. D.[1]

1. Department of Orthopaedic Surgery, Faculty of Medicine and Graduate School of Medicine, Hokkaido University, Sapporo, Japan
2. Department of Functional Reconstruction for the Knee Joint, Faculty of Medicine, Hokkaido University, Sapporo, Japan
3. Centre for Sports Medicine, Hokkaido University Hospital, Sapporo, Japan

Corresponding author
- Koji Iwasaki, MD, PhD.
- Institutional address: North-15, West-7, Sapporo, Hokkaido 060-8638, Japan
- Phone: +81-11-706-5934
- Email: kojiwasaki@pop.med.hokudai.ac.jp

1 **Abstract**

2 **Purpose** Anterior cruciate ligament (ACL) injury induces anterior and rotatory instability

3 of the knee. However, the effect of this instability on the stress distribution in the knee

4 joint in living participants is not clear. The aim of this study was to compare the

5 distribution pattern of subchondral bone density across the proximal tibia in the knees

6 with and without ACL injury, and to investigate the correlation between the distribution

7 patterns of the subchondral bone density and the duration of ACL-deficiency.

8 **Methods** Radiographic and computed tomography (CT) data pertaining to 20 patients

9 with unilateral ACL injury without combined injury (ACL-deficient group) and 19

10 nontraumatic subjects (control group) were collected retrospectively. Subchondral bone

11 density of the proximal tibia was assessed using CT-osteoabsorptiometry. Both the medial

12 and lateral compartments of the proximal tibia were divided into three subregions of equal

13 width in the sagittal direction. The percentage of high subchondral bone density areas

14 (HDA%) in each subregion was quantitatively analyzed.

15 **Results** HDA% of the posteromedial region was significantly higher in the ACL-deficient

16 group (mean: 21.6%) than in the control group (14.7%) ($p = 0.002$). In contrast, HDA%

17 of the anteromedial region was significantly lower in the ACL-deficient group (9.4%)

18 than in the control group (15.3%) ($p = 0.048$). The logarithm of the time elapsed from

19 ACL injury to CT examination showed a significant correlation with HDA% in the

20 posteromedial region ($p = 0.032$).

21 **Conclusions** Subchondral bone density in the posteromedial region significantly

22 increased after ACL injury and correlated with the duration of ACL-deficiency in semi-

23 log manner in meniscus intact knees. The increase in stress on the posteromedial region

24 after ACL injury, which induces a change in the subchondral bone density, justifies early

25 ACL reconstruction after ACL injury.

26

INTRODUCTION

Anterior cruciate ligament (ACL) injury induces anterior and rotatory instability of the knee, which affects the performance level of athletes; moreover, this instability may cause knee buckling or giving way even in non-athletes. Anterior and rotatory instability is known to alter the positional relationship between the distal femur and the proximal tibia [4, 11, 26, 28, 34, 43]. This instability after ACL injury is believed to lead to abnormal stress distribution across the knee joint [6, 9, 12, 42]. In cadaveric studies, the contact stress on the posteromedial part of the proximal tibial articular surface in response to anterior tibial load was found to be higher in ACL-deficient knee than in the intact knee [6, 42]. In addition, the location of the common dynamic stress distribution on the proximal tibial articular surface changed after ACL transection during simulated gait [9].

However, it is technically challenging to measure the actual stress distribution across the knee joint in the ACL-deficient knee. Moreover, whether and how the actual in vivo stress distribution changes after ACL injury is not well characterized.

Computed tomography (CT)-osteoabsorptiometry is an analytical method for in vivo assessment of the stress distribution at joints through the subchondral bone density. It has been demonstrated by our previous studies that CT-osteoabsorptiometry is a useful method for evaluation of in vivo stress distribution in various joints [15, 19-21, 23, 32,

45   33].

46   It was hypothesized that the stress distribution pattern of the proximal tibial

47   articular surface would change over time after ACL injury. The purpose of this study was

48   (1) to compare the distribution pattern of subchondral bone density across the proximal

49   tibia with and without ACL injury, and (2) to clarify the influence of the duration of ACL

50   deficiency on the distribution of subchondral bone density. Using CT-osteoabsorptiometry,

51   the change in stress distribution within each compartment of the proximal tibia after ACL

52   injury and the influence of the time elapsed after ACL injury on the stress distribution

53   across the knee joint could be elucidated by this study.

54

55   **MATERIAL AND METHODS**

56   This study protocol was approved by the institutional review board of Hokkaido

57   University Hospital (IRB number, 017-0163). Analysis was conducted by retrospectively

58   evaluating the preoperative CT scans of the knees of patients who underwent ACL

59   reconstruction between 2016 and 2019 at our institution. Inclusion criteria were patients

60   who had unilateral ACL injury and had undergone CT and MRI examination prior to ACL

61   reconstruction. The exclusion criteria were: (1) meniscal injury which was found in

62   preoperative MRI images ($\geq$ grade II, according to Lotysch and Mink's MRI evaluation

63   system [29]) or that was diagnosed by arthroscopic examination during the ACL

64   reconstruction surgery; (2) cartilage injury (≥International Cartilage Repair Society

65   [ICRS] grade II [8, 18]); (3) osteoarthritis (≥ Kellgren-Laurence [KL] grade II [24]); (4)

66   concomitant chondral injury or ligament injury detected by preoperative MRI or

67   arthroscopic evaluation; (5) age >35 years (Figure 1). In total, 70 patients were diagnosed

68   with ACL injury during the study's data collection period at our institution. Of those, 50

69   patients were excluded, and the remaining 20 patients were included in the study as those

70   having ACL-deficient knees (ACL-deficient group) (Figure 1). In addition, for

71   comparison of ipsilateral knee trauma, we collected the data of patients undergoing

72   simultaneous radiographic and CT examinations of the bilateral knees between 2015 and

73   2019; these patients were considered control subjects. Inclusion criteria for the control

74   group were: (1) osteoarthritis (KL grade ≤ 1) in the contralateral knee, (2) age <35 years

75   at the time of CT, and (3) no trauma history. Nineteen uninjured contralateral knees were

76   used as controls. There were no significant differences in age, sex, HKA angle, PTS angle,

77   and Tegner activity scale score between the control and ACL-deficient groups (Table 1).

78

79   **Clinical and radiological evaluation**

80   In the ACL-deficient group, the side-to-side differences of the anterior laxity were

81 measured with a KT-2000 arthrometer (MED metric, San Diego, CA, USA) at 30° of knee

82 flexion under an anterior drawer force of 133 N. For radiological evaluation, bilateral

83 standing anteroposterior (AP), lateral views of the knee, and full-length AP radiographs

84 of the whole lower limb in full extension were assessed. Tibiofemoral osteoarthritis was

85 evaluated according to the KL grading system, Hip-knee-ankle (HKA) angle, and

86 posterior tibial slope (PTS) angle. The PTS was defined as the angle between the line

87 perpendicular to the mid-diaphysis of the tibia and the posterior inclination of the medial

88 tibial plateau. Patient activity before ACL injury was evaluated using the Tegner activity

89 scale [40].

90 **Computed tomography–osteoabsorptiometry**

91 A high-resolution helical CT scanner (Aquilion One/ViSION Edition; Toshiba Medical

92 Systems, Japan) was used to acquire axial images of the knee in full extension. Slice

93 thickness and interval were set at 0.5 mm. The acquired CT data were transferred to a

94 personal computer. The sagittal and coronal slices at 1.0-mm intervals and 3-D bone

95 models were generated from axial CT data using a commercial software (Ziocube®;

96 Ziosoft, Inc., Tokyo, Japan). The sagittal and coronal axes were determined with reference

97 to the epicondylar axis of the distal femoral condyle in the axial slice. By referring to

98 sagittal and coronal CT images and a 3-D CT image of the articular surface of the

99   proximal tibia, an outline of the medial and lateral compartment of the proximal tibial

100   articular surface was manually selected to include the entire subchondral bone layer of

101   the articular surface in all slices [20]. Subsequently, the subchondral bone density of each

102   generated sagittal slice was analyzed using an original non-commercial software

103   (OsteoDens 4.0) developed at our institution [15, 19, 20, 23, 32, 33]. The maximum

104   increment point in Hounsfield units from the joint surface was set as the starting point of

105   the region of interest, and the maximum point in Hounsfield units was selected

106   automatically in the 2.5-mm region of interest from the starting point [20]. We determined

107   the radiodensity of the identified subchondral bone region at each coordinate point at 1.0-

108   mm intervals. Subsequently, a two-dimensional image that mapped the distribution of

109   subchondral bone density was obtained by stacking the sagittal slices (Figure 2A, 2B).

110   The differences between the maximum and minimum values (in Hounsfield units [HU])

111   on the mapping images were categorized into nine grades; subsequently, a surface

112   mapping image was generated using these grades to produce a color scale in which red

113   and violet indicated the greatest and lowest bone densities, respectively. The selected

114   areas of the medial and lateral plateaus included the cortical bone at the periphery of the

115   articular surface because it was impossible to exclude the cortical bone using the software.

116   However, these features were manually removed from the target area of analysis in the

117 subsequent quantitative analysis [20].

118   Quantitative analysis of the obtained mapping data focused on the location of the

119 high-density area (HDA) of the articular surface. The HDA was defined as the region

120 containing the coordinate points representing the top 30% area of HU values in each

121 medial or lateral compartment. The medial compartment of the proximal tibia was divided

122 into three subregions of equal width in the sagittal direction, denoted anteromedial (AM),

123 centromedial (CM), and posteromedial (PM) from anterior to posterior. The lateral

124 compartment was similarly divided into anterolateral (AL), centrolateral (CL), and

125 posterolateral (PL) from anterior to posterior (Figure 2C). The percentage of each

126 subregion represented by the HDA (HDA%) was calculated (see Supplemental File). The

127 measurement results in this study are presented to one decimal place of precision.

128 Quantitative analysis was performed in a blinded manner by two observers (## and ##).

129 The same set of images was measured by each examiner after 4 weeks. The averages of

130 these measurements were used in our analysis.

131   The reproducibility of data was evaluated using OsteoDens 4.0 software. Intra-

132 and interobserver reliability were assessed using three randomly selected knees from the

133 control group and ACL-deficient group. HDA% was measured independently by two

134 observers (KI and SM) in these six knees; a total of 36 subregions were measured twice

135   in a blinded manner at 4-week intervals. The intraclass correlation coefficients for

136   intraobserver reliability were 0.88 (KI) and 0.91 (SM), respectively, and the intraclass

137   correlation coefficient for interobserver reproducibility was 0.87.

138   **Statistical analysis**

139   Statistical analyses were performed using JMP Pro 14.0 (SAS Institute Inc., Cary, NC,

140   USA). $P < 0.05$ was considered statistically significant. Comparisons between control

141   and ACL-deficient groups were performed using the Student's t test or the chi-square test.

142   Pearson's correlation coefficient was used to examine the relationship between HDA% in

143   each subregion and other variables, including anterior laxity, period from ACL injury to

144   CT, HKA angle, and PTS angle, because they are believed to influence the distribution of

145   subchondral bone density [22, 36, 41] or the biomechanics of the knee joint [3, 35]. Post

146   hoc power analysis revealed that for an alpha value of 0.05, a power of 0.96 on a sample

147   size of 20 knees was achieved for the difference in HDA% in the PM region.

148

149   **RESULTS**

150

151   **HDA% in each subregion**

152   HDA% of the posteromedial region in the ACL-deficient group was 7% higher than in

153   the control group ($p = 0.002$). In contrast, HDA% of the anteromedial region in the ACL-

154   deficient was 6% lower than in the control group ($p = 0.048$). There were no significant

155   differences in HDA% of centromedial region and subregions of the lateral compartment

156   between the ACL-deficient and control groups (Table 2).

157

158   **Correlation between HDA% and other variables**

159   HDA% of the posteromedial region showed no correlation with the time elapsed from

160   ACL injury to CT examination (n.s., r = 0.288), but showed a significant correlation with

161   the logarithm of the time elapsed from ACL injury to CT examination ($p = 0.032$. r =

162   0.480) (Figure 3). HDA% of the anteromedial region showed no correlation with the time

163   elapsed either on the arithmetic plot or the semi-log plots. HDA% of the posteromedial

164   region showed no correlation with other variables, including anterior laxity, HKA angle,

165   and PTS angle.

166

167   **DISCUSSION**

168   The main findings of the present study were that HDA% of the posteromedial region of

169   the proximal tibia in the ACL-deficient group with intact meniscus was significantly

170   higher than that in the control group Furthermore, HDA% of the posteromedial region

171   showed a significant correlation with the duration of ACL-deficiency on semi-log curves.

172   Previous studies involving CT-osteoabsorptiometry have indicated that the

173   distribution pattern of subchondral bone density reflects the distribution of the stress

174   acting on the joint surface under actual loading conditions [19-21, 23, 31-33]. Funakoshi

175   et al. found high-stress distribution patterns on the anterolateral part of the capitellum and

176   the anterolateral part of the ulna in symptomatic patients with ulnar collateral ligament

177   insufficiency [15]. Therefore, CT-osteoabsorptiometry can help assess the *in vivo* stress

178   distribution across the ACL-deficient knee joint. In the present study, HDA% in the

179   posteromedial region of the proximal tibia was found to be higher in the ACL-deficient

180   knees than in the normal knees. This result suggests that ACL injury increased the stress

181   on the posteromedial region of the proximal tibia, since the changes in subchondral bone

182   density are believed to result from changes in stress distribution. Experimental studies

183   using animal models, ACL transection induced progression of osteoarthritis over time [1,

184   7, 13]. These results suggested that chronic ACL-deficiency leads to accumulation of

185   stress, which causes the initiation and progression of osteoarthritis (OA) [5]. These

186   speculations were supported by our findings in the present study.

187   There was a positive correlation between the logarithm of the time elapsed since

188   ACL-deficiency and HDA% of the posteromedial region in the meniscus intact knees.

189   These results suggested that stress on the posteromedial region increased rapidly after

190   ACL injury and was accumulated gradually over time, while the meniscus was intact.

191   These findings suggested that patients with ACL injury should undergo ACL

192   reconstruction as soon as possible from the perspective of aggressive prevention of

193   osteoarthritis, even though the meniscus was not injured.

194   There are several potential mechanisms of the changes in stress distribution after

195   ACL injury including anterior translation of the tibia relative to the femoral condyle [11,

196   26, 28, 42] and anterolateral rotatory instability [11, 26, 34, 42]. Furthermore, three-

197   dimensional gait analyses revealed reduced internal rotational moment in ACL-deficient

198   knees during the terminal stance phase. This gait pattern was described as a "pivot-shift

199   avoidance gait" [14, 38]. Theoretically, anterior translation is believed to increase the

200   stress on the posteromedial region of the tibial plateau and decrease the stress on the

201   anteromedial region because of the concave shape of the medial tibial plateau. In addition,

202   internal rotatory instability may decrease the stress on the posteromedial region of the

203   tibial plateau and increase the stress on the anteromedial region. "Pivot shift avoidance

204   gait" may affect reciprocally compared to rotatory instability. This study suggested that

205   ACL injury increased the stress on the posteromedial region without any correlation with

206   the extent of anterior instability and PTS; in addition, ACL injury led to decreased stress

207   on the anteromedial region. Taking into account both the assumed mechanisms affecting

208   the stress distribution and the obtained results in the anteromedial and posteromedial

209   region, anterior translation is believed to be the main mechanism of the altered stress

210   distribution. Furthermore, internal rotation may not counteract the effect of anterior

211   translation on the stress distribution, or "pivot shift avoidance gait" may play an important

212   role in the stress distribution compared to internal rotation after ACL injury.

213   A quasi-static and dynamic biomechanical cadaveric study revealed increase of

214   dynamic contact stress on the posterior lateral tibial plateau [9], indicating that the

215   posterior tibial plateau hit against lateral femoral condyle when tibia rotated internally. In

216   the present study, we found no evidence of increased stress on the posterior lateral tibial

217   plateau. CT-OAM method indicated the resultant stress through the distribution pattern

218   of subchondral bone density across the joint, reflecting all movements including not only

219   walking but the compensatory movement against internal rotatory instability. Thus, these

220   differences in the speculation of the stress distribution between the dynamic

221   biomechanical cadaveric study and this CT-OAM study demonstrated a compensatory

222   movement against rotatory instability, which could not be simulated by the knee simulator

223   [9].

224   Leg alignment has been reported to strongly influence the distribution of

225 subchondral bone density between the medial and lateral compartments of the proximal

226 tibia [2, 17, 41], indicating that leg alignment counteracted a change in the distribution of

227 subchondral bone density in the sagittal direction due to knee instability. Our previous

228 study demonstrated that the relative value of subchondral bone density in eight sub-

229 regions in the coronal direction among subjects increased significantly, up to 6%, and

230 shifted laterally after high tibial osteotomy (HTO) [20]. Therefore, in the present study,

231 we used the relative value of bone density within compartments in the sagittal direction

232 to detect a change in subchondral bone density distribution in the sagittal direction after

233 ACL injury. Consequently, there was a 5% decrease in the relative value of bone density,

234 compared with the control group, in the anteromedial region and an increase of 6% in the

235 posteromedial region after ACL injury, demonstrating a rearward shift of subchondral

236 bone density distribution. Taking into account the drastic change in knee biomechanics

237 before and after HTO, 5%–6% differences in the relative value of bone density in the

238 sagittal direction between ACL-deficient and control groups was thought to be a

239 substantial change. Although clinical evaluation was not performed in this study, the

240 rearward shift of stress distribution, which induced the rearward shift of subchondral bone

241 density distribution, has been reported to be a cause of the high incidence of medial

242 meniscus injury in chronically ACL-deficient knees [16, 39].

243   In addition to leg alignment, patient activity level and PTS angle could have

244   affected bone density. ACL injuries tend to affect individuals with a high activity level,

245   which could have an impact on bone density [30, 37], and PTS angle was associated with

246   knee instability in ACL-deficient knees [10]. However, there were no significant

247   differences in the activity level and PTS angle between the control and ACL-deficient

248   groups in our study. Therefore, those factors may not have contributed to the difference

249   between the ACL-deficient and control groups.

250   Regarding the influence of the initial injury itself on the bone density, ACL injury

251   is usually provoked by internal rotation and anterior translation, resulting mainly in bone

252   bruising at the posterior wall of the lateral tibial plateau [25, 43]. The posterior wall of

253   the lateral tibial plateau is outside the region of interest in the CT-OAM method. The

254   metaphyseal part of the proximal tibia is too deep to assess by CT-OAM. Furthermore,

255   HDA% of the posterolateral region was not significantly changed in the ACL-deficient

256   group compared to that in the control group. Thus, initial injury may not influence the

257   distribution of subchondral bone density assessed by the CT-OAM method.

258   In addition, the effect of any instability immediately after ACL injury on

259   subchondral bone density might be minimal; however, in a previous study, a 10%

260   decrease in the absolute BMD of the proximal tibia was seen 100 days after ACL injury

261 with reduced mobility and low activity [27]. Our results of a significant change in the

262 relative value of subchondral bone density in the posteromedial region 90 days after ACL

263 injury may be supported by this change in absolute BMD after ACL injury.

264   Some limitations of our study should be considered when interpreting the

265 findings. First, the stress was not measured directly but through the distribution of

266 subchondral bone density based on the CT-OAM findings [31]. Furthermore, the absolute

267 value of BMD was not evaluated; instead, the relative value in each subregion of each

268 compartment was evaluated. It should be noted that the stress distribution evaluated by

269 the CT-OAM method may not reflect the actual stress. Second, this study lacked a

270 standardized rehabilitation protocol and level of rest. Despite these limitations, the

271 strength of this study was that we matched the two groups with respect to factors that may

272 influence the distribution pattern of subchondral bone density (including age, BMI, and

273 geometry of knee). Thus, a basic clarification that in vivo stress distribution changes over

274 time after ACL surgery is demonstrated by our results.

275

276 **CONCLUSION**

277 It has been demonstrated that HDA of the posteromedial region of the proximal tibia in

278 ACL-deficient knees was significantly higher than that in ACL-intact knees. Moreover, it

279   was found that HDA of the posteromedial region was correlated with the duration of ACL

280   deficiency on semi-log plots. The increase in stress on the posteromedial region over time

281   after ACL injury, which induces a change in the subchondral bone density, provides

282   orthopedic surgeons with a justification for early ACL reconstruction after ACL injury.

283

284   **Acknowledgements**

286

REFERENCES

1. Adams ME, Brandt KD (1991) Hypertrophic repair of canine articular cartilage in osteoarthritis after anterior cruciate ligament transection. J Rheumatol 18:428-435

2. Akamatsu Y, Koshino T, Saito T, Wada J (1997) Changes in osteosclerosis of the osteoarthritic knee after high tibial osteotomy. Clin Orthop Relat Res 334:207-214

3. Andriacchi TP, Briant PL, Bevill SL, Koo S (2006) Rotational changes at the knee after ACL injury cause cartilage thinning. Clin Orthop Relat Res 442:39-44

4. Andriacchi TP, Dyrby CO (2005) Interactions between kinematics and loading during walking for the normal and ACL deficient knee. J Biomech 38:293-298

5. Andriacchi TP, Mundermann A (2006) The role of ambulatory mechanics in the initiation and progression of knee osteoarthritis. Curr Opin Rheumatol 18:514-518

6. Bedi A, Chen T, Santner TJ, El-Amin S, Kelly NH, Warren RF, et al. (2013) Changes in dynamic medial tibiofemoral contact mechanics and kinematics after injury of the anterior cruciate ligament: a cadaveric model. Proc Inst Mech Eng H 227:1027-1037

7. Brandt KD, Braunstein EM, Visco DM, O'Connor B, Heck D, Albrecht M (1991) Anterior (cranial) cruciate ligament transection in the dog: a bona fide model of osteoarthritis, not merely of cartilage injury and repair. J Rheumatol 18:436-446

8. Brittberg M, Winalski CS (2003) Evaluation of cartilage injuries and repair. J Bone Joint Surg Am 85-A Suppl 2:58-69

9. Chen T, Wang H, Warren R, Maher S (2017) Loss of ACL function leads to alterations in tibial plateau common dynamic contact stress profiles. J Biomech 61:275-279

10. Dejour D, Pungitore M, Valluy J, Nover L, Saffarini M, Demey G (2019) Preoperative laxity in ACL-deficient knees increases with posterior tibial slope and medial meniscal tears. Knee Surg Sports Traumatol Arthrosc 27:564-572

11. Dennis DA, Mahfouz MR, Komistek RD, Hoff W (2005) In vivo determination of normal and anterior cruciate ligament-deficient knee kinematics. J Biomech 38:241-253

12. Du PZ, Markolf KL, Boguszewski DV, McAllister DR (2018) Femoral Contact Forces in the Anterior Cruciate Ligament Deficient Knee: A Robotic Study. Arthroscopy 34:3226-3233

13. Fischenich KM, Button KD, Coatney GA, Fajardo RS, Leikert KM, Haut RC, et al. (2015) Chronic changes in the articular cartilage and meniscus following traumatic impact to the lapine knee. J Biomech 48:246-253

14. Fuentes A, Hagemeister N, Ranger P, Heron T, de Guise JA (2011) Gait adaptation in chronic anterior cruciate ligament-deficient patients: Pivot-shift avoidance gait. Clin Biomech (Bristol, Avon) 26:181-187

15. Funakoshi T, Furushima K, Momma D, Endo K, Abe Y, Itoh Y, et al. (2016) Alteration of Stress

322   Distribution Patterns in Symptomatic Valgus Instability of the Elbow in Baseball Players: A

323   Computed Tomography Osteoabsorptiometry Study. Am J Sports Med 44:989-994

324   16.   Hagino T, Ochiai S, Senga S, Yamashita T, Wako M, Ando T, et al. (2015) Meniscal tears

325   associated with anterior cruciate ligament injury. Arch Orthop Trauma Surg 135:1701-1706

326   17.   Han X, Cui J, Xie K, Jiang X, He Z, Du J, et al. (2020) Association between knee alignment,

327   osteoarthritis disease severity, and subchondral trabecular bone microarchitecture in patients with

328   knee osteoarthritis: a cross-sectional study. Arthritis Res Ther 22:203

329   18.   Hjelle K, Solheim E, Strand T, Muri R, Brittberg M (2002) Articular cartilage defects in 1,000

330   knee arthroscopies. Arthroscopy 18:730-734

331   19.   Irie T, Takahashi D, Asano T, Arai R, Terkawi MA, Ito YM, et al. (2018) Is There an Association

332   Between Borderline-to-mild Dysplasia and Hip Osteoarthritis? Analysis of CT

333   Osteoabsorptiometry. Clin Orthop Relat Res 476:1455-1465

334   20.   Iwasaki K, Kondo E, Matsubara S, Matsuoka M, Endo K, Yokota I, et al. (2021) Effect of High

335   Tibial Osteotomy on the Distribution of Subchondral Bone Density Across the Proximal Tibial

336   Articular Surface of the Knee With Medial Compartment Osteoarthritis. Am J Sports Med

337   49:1561-1569

338   21.   Iwasaki N, Minami A, Miyazawa T, Kaneda K (2000) Force distribution through the wrist joint in

339   patients with different stages of Kienbock's disease: using computed tomography

340   osteoabsorptiometry. J Hand Surg Am 25:870-876

341   22.   Johnston JD, Masri BA, Wilson DR (2009) Computed tomography topographic mapping of

342   subchondral density (CT-TOMASD) in osteoarthritic and normal knees: methodological

343   development and preliminary findings. Osteoarthritis Cartilage 17:1319-1326

344   23.   Kameda T, Kondo E, Onodera T, Iwasaki K, Onodera J, Yasuda K, et al. (2021) Changes in the

345   Contact Stress Distribution Pattern of the Patellofemoral Joint After Medial Open-Wedge High

346   Tibial Osteotomy: An Evaluation Using Computed Tomography Osteoabsorptiometry. Orthop J

347   Sports Med 9:2325967121998050

348   24.   Kellgren JH, Lawrence JS (1957) Radiological assessment of osteo-arthrosis. Ann Rheum Dis

349   16:494-502

350   25.   Kim-Wang SY, Scribani MB, Whiteside MB, DeFrate LE, Lassiter TE, Wittstein JR (2021)

351   Distribution of Bone Contusion Patterns in Acute Noncontact Anterior Cruciate Ligament-Torn

352   Knees. Am J Sports Med 49:404-409

353   26.   Kondo E, Merican AM, Yasuda K, Amis AA (2010) Biomechanical comparisons of knee stability

354   after anterior cruciate ligament reconstruction between 2 clinically available transtibial

355   procedures: anatomic double bundle versus single bundle. Am J Sports Med 38:1349-1358

356   27.   Kroker A, Besler BA, Bhatla JL, Shtil M, Salat P, Mohtadi N, et al. (2019) Longitudinal Effects

357   of Acute Anterior Cruciate Ligament Tears on Peri-Articular Bone in Human Knees Within the

| 358 | | First Year of Injury. J Orthop Res 37:2325-2336 |
359	28.	Kvist J (2004) Sagittal plane translation during level walking in poor-functioning and well-
360		functioning patients with anterior cruciate ligament deficiency. Am J Sports Med 32:1250-1255
361	29.	Lotysch M, Mink J, Crues JV, Schwartz SA (1986) Magnetic resonance imaging in the detection
362		of meniscal injuries. Magn Reson Imaging 4:185
363	30.	Momma D, Iwamoto W, Endo K, Sato K, Iwasaki N (2020) Stress Distribution Patterns Across
364		the Shoulder Joint in Gymnasts: A Computed Tomography Osteoabsorptiometry Study. Orthop J
365		Sports Med 8:2325967120962103
366	31.	Muller-Gerbl M, Putz R, Hodapp N, Schulte E, Wimmer B (1989) Computed tomography-
367		osteoabsorptiometry for assessing the density distribution of subchondral bone as a measure of
368		long-term mechanical adaptation in individual joints. Skeletal Radiol 18:507-512
369	32.	Nishida K, Iwasaki N, Fujisaki K, Funakoshi T, Kamishima T, Tadano S, et al. (2012) Distribution
370		of bone mineral density at osteochondral donor sites in the patellofemoral joint among baseball
371		players and controls. Am J Sports Med 40:909-914
372	33.	Onodera T, Majima T, Iwasaki N, Kamishima T, Kasahara Y, Minami A (2012) Long-term stress
373		distribution patterns of the ankle joint in varus knee alignment assessed by computed tomography
374		osteoabsorptiometry. Int Orthop 36:1871-1876
375	34.	Scarvell JM, Smith PN, Refshauge KM, Galloway HR, Woods KR (2004) Comparison of
376		kinematic analysis by mapping tibiofemoral contact with movement of the femoral condylar
377		centres in healthy and anterior cruciate ligament injured knees. J Orthop Res 22:955-962
378	35.	Schatka I, Weiler A, Jung TM, Walter TC, Gwinner C (2018) High tibial slope correlates with
379		increased posterior tibial translation in healthy knees. Knee Surg Sports Traumatol Arthrosc
380		26:2697-2703
381	36.	Sharma L (2001) Local factors in osteoarthritis. Curr Opin Rheumatol 13:441-446
382	37.	Shiota J, Momma D, Yamaguchi T, Iwasaki N (2020) Long-term Stress Distribution Patterns
383		Across the Ankle Joint in Soccer Players: A Computed Tomography Osteoabsorptiometry Study.
384		Orthop J Sports Med 8:2325967120963085
385	38.	Takeda K, Hasegawa T, Kiriyama Y, Matsumoto H, Otani T, Toyama Y, et al. (2014) Kinematic
386		motion of the anterior cruciate ligament deficient knee during functionally high and low
387		demanding tasks. J Biomech 47:2526-2530
388	39.	Tashiro Y, Mori T, Kawano T, Oniduka T, Arner JW, Fu FH, et al. (2020) Meniscal ramp lesions
389		should be considered in anterior cruciate ligament-injured knees, especially with larger instability
390		or longer delay before surgery. Knee Surg Sports Traumatol Arthrosc 28:3569-3575
391	40.	Tegner Y, Lysholm J (1985) Rating systems in the evaluation of knee ligament injuries. Clin
392		Orthop Relat Res 198:43-49
393	41.	Wada M, Maezawa Y, Baba H, Shimada S, Sasaki S, Nose Y (2001) Relationships among bone

394   mineral densities, static alignment and dynamic load in patients with medial compartment knee

395   osteoarthritis. Rheumatology (Oxford) 40:499-505

396   42.   Wang D, Kent RN, 3rd, Amirtharaj MJ, Hardy BM, Nawabi DH, Wickiewicz TL, et al. (2019)

397   Tibiofemoral Kinematics During Compressive Loading of the ACL-Intact and ACL-Sectioned

398   Knee: Roles of Tibial Slope, Medial Eminence Volume, and Anterior Laxity. J Bone Joint Surg

399   Am 101:1085-1092

400   43.   Willinger L, Athwal KK, Williams A, Amis AA (2021) An Anterior Cruciate Ligament In Vitro

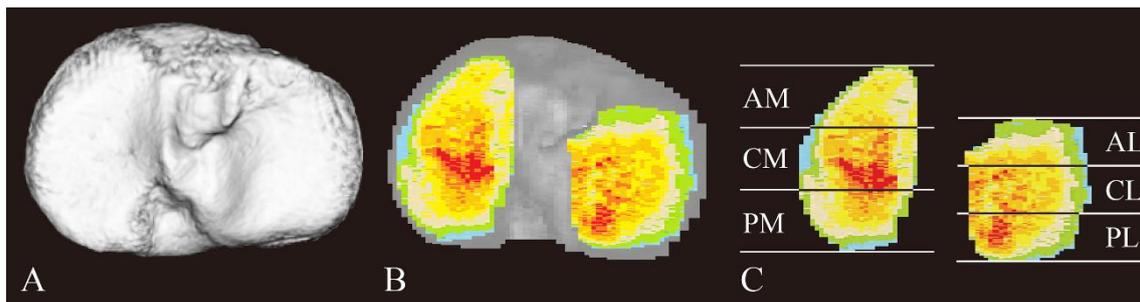401   Rupture Model Based on Clinical Imaging. Am J Sports Med 49:2387-2395

402

FIGURE LEGENDS
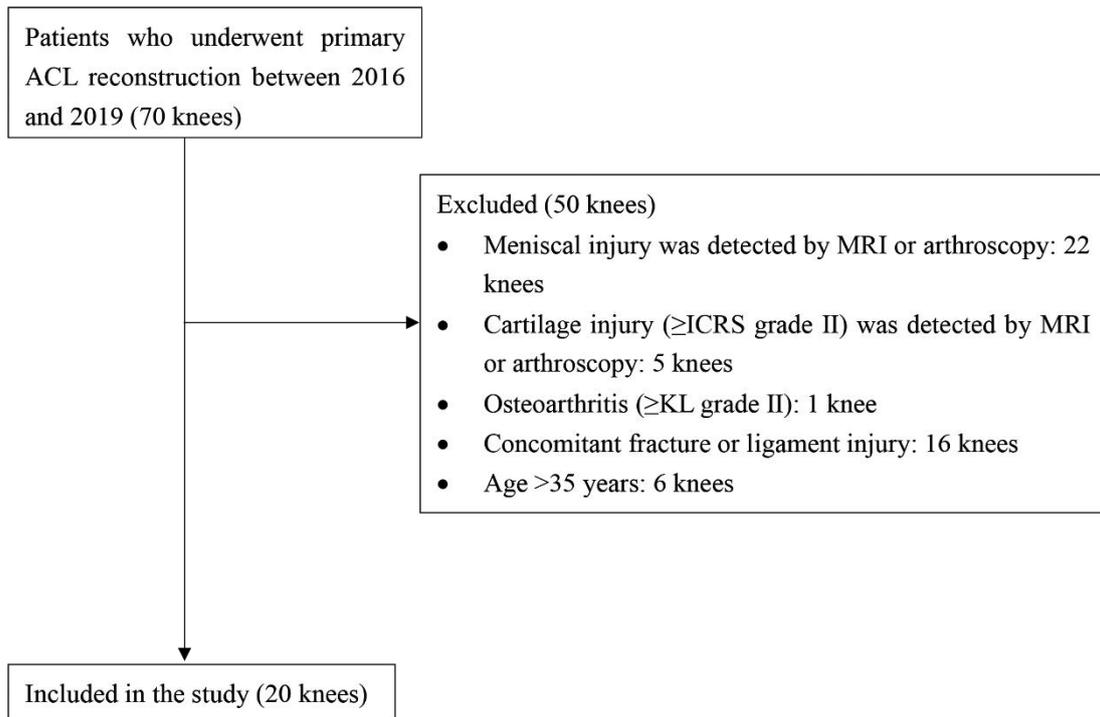
405 **Figure 1.** Flowchart of study enrollment. ICRS, International Cartilage Regeneration &

406 Joint Preservation Society-Cartilage Repair Assessment system; KL, Kellgren-Laurence.


407

408 **Figure 2.** Identification of the subchondral bone regions of the proximal tibia using a

409 customized software. (A, B) The subchondral bone density of the selected region was

410 automatically measured at each coordinate point in each 1.0-mm sagittal slice. (C) Both

411 the medial and lateral compartments of the tibial articular surface were divided into three

412   subregions each from anterior to posterior for quantitative analysis of the distribution of

413   high subchondral bone density area

414   AM, anteromedial; CM, centromedial; PM, posteromedial; AL, anterolateral; CL,

415   centrolateral; PL, posterolateral

(%)

P = 0.032
r = 0.480

416
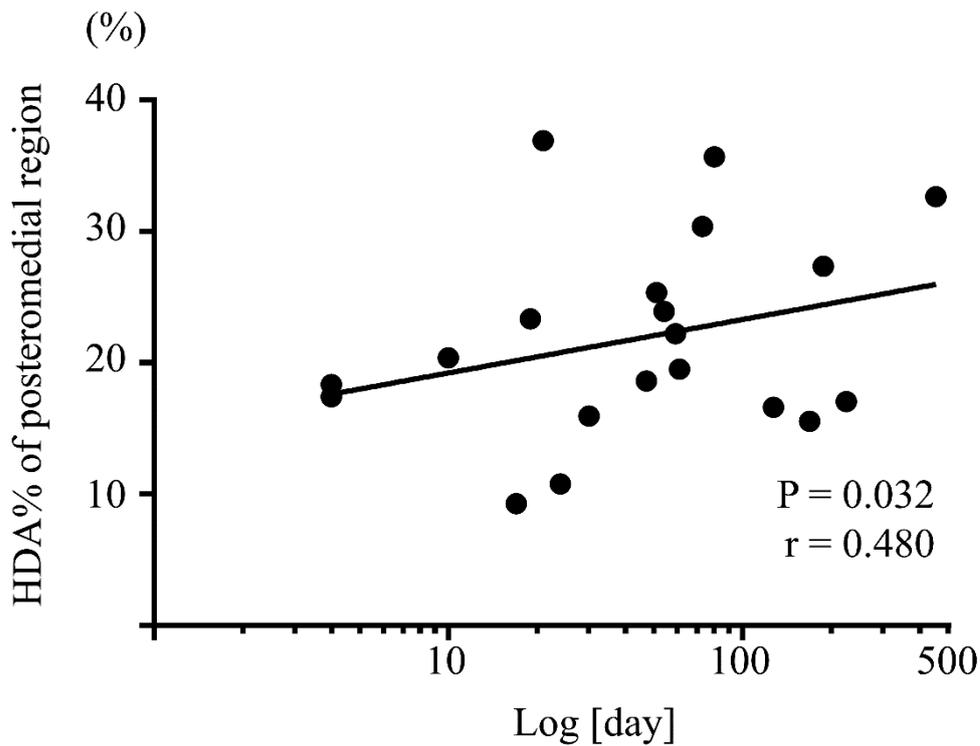
Figure 3. Semi-log plots of the time elapsed from ACL injury vs. HDA% in the

posteromedial region of the proximal tibia

ACL, anterior cruciate ligament; HDA%, percentage of high subchondral bone density

area

Table 1. Characteristics of the study population[a]

	Control group (n = 19)	ACLD group (n = 20)	*p* value
Age, years	23.4 (21.3–26.5)	21.5 (18.5–23.6)	n.s.
Male:Female, n	10:9	10:10	n.s.
BMI, kg/m^2	24.1 (21.8–26.5)	24.3 (22.3–26.2)	n.s.
Anterior laxity, mm	n/a	3.2 (1.8–4.5)	n/a
Period from ACL injury to CT examination, days	n/a	91.4 (35.8–146.9)	n/a
HKA angle, degrees	−0.5 (−2.6–1.6)	−0.3 (−1.8–1.3)	n.s.
PTS angle, degrees	10.4 (8.6–12.2)	10.7 (8.9–12.5)	n.s.
Tegner activity scale score	6.9 (6.1–7.7)	6.4 (5.5–7.2)	n.s.

423 [a]Data presented as frequency or mean (95% confidence interval).

424 ACL, anterior cruciate ligament; ACLD, anterior cruciate ligament deficient; Anterior
425 laxity: side-to-side anterior knee laxity at 30° flexion, BMI, body mass index; CT,
426 computed tomography; HKA, hip-knee-ankle; n/a, not applicable; n.s., not significant;
427 PTS, posterior tibial slope.

428

429 **Table 2. Quantitative analysis of HDA% in each subregion[a]**

		Control group	ACLD group	*p* value
Medial compartment (%)	AM	15.3 (9.6–21.0)	9.4 (6.8–12.0)	0.048
	CM	52.0 (47.8–56.3)	52.4 (49.3–55.5)	n.s.
	PM	14.7 (12.5–17.0)	21.6 (18.0–25.3)	0.002
Lateral compartment (%)	AL	3.1 (1.2–5.0)	2.7 (1.3–4.1)	n.s.
	CL	38.2 (34.6–41.9)	38.9 (36.4–41.4)	n.s.

	PL	43.1 (38.4–47.8)	44.7 (40.2–49.1)	n.s.

430 [a]Data presented as mean (95% confidence interval)

431 ACLD, anterior cruciate ligament deficient; AL, anterolateral; AM, anteromedial; CL,

432 centrolateral; CM, centromedial; HDA%, percentage of high subchondral bone density

433 area; n.s., not significant; PL, posterolateral; PM, posteromedial.

434